



Green
Chemistry

**Synthesis and Properties of Linseed Oil-Based Waterborne
Non-isocyanate Polyurethane Coating**

Journal:	<i>Green Chemistry</i>
Manuscript ID	GC-ART-08-2023-003249.R1
Article Type:	Paper
Date Submitted by the Author:	03-Nov-2023
Complete List of Authors:	Ling, Zichen; University of Akron Zhou, Qixin; The University of Akron, Department of Chemical, Biomolecular, and Corrosion Engineering

SCHOLARONE™
Manuscripts

Synthesis and Properties of Linseed Oil-Based Waterborne Non-isocyanate Polyurethane Coating

Zichen Ling, Qixin Zhou *

Department of Chemical, Biomolecular, and Corrosion Engineering, The University of Akron,
Akron, Ohio, 44325, United States

*: corresponding author

E-mail: qzhou@uakron.edu

Abstract

Significant strides in the development of non-isocyanate polyurethane (NIPU) have been made in the coatings industry. Aligned with green chemistry principles, this study explores the use of bio-based, low volatile organic compounds and fast-curing waterborne NIPU for coating applications. The linseed oil-based cyclic carbonate was synthesized via a thiol-ene click reaction and was followed by an esterification reaction directly from linseed oil. In this structure, the cyclic carbonates are introduced as pendant functional groups to accelerate the curing. Next, a series of linseed oil-based waterborne NIPUs were synthesized and developed from the linseed oil-based cyclic carbonate, a bio-based fatty acid diamine, and an internal dispersion agent. Different formulations of the linseed oil-based NIPU coatings were designed by varying the internal dispersion agent content and urethane content, and a solvent-borne NIPU was included in the study for comparison purposes. The NIPU coatings with different formulations achieved a broad range of thermal stabilities, viscoelastic properties, and

mechanical properties. The general coating properties—including hardness, solvent resistance, impact resistance, and adhesion—were evaluated to demonstrate the practical application of the waterborne NIPU in coatings. The linseed oil-based waterborne NIPU coatings exhibited performance comparable to both a solvent-borne NIPU coating and a commercial waterborne isocyanate-based polyurethane coating.

Introduction

Polyurethane (PU) is a versatile material used in many applications such as sensors, medical dressings, food packaging, foams, and coatings¹⁻⁵; the global market for this material was valued at over \$70 billion in 2021 and is expected to increase at a rate of 4.5% per year⁶. In general, traditional PU shows excellent properties because of the presence of hydrogen bonding and alternately arranged soft and hard segments⁷, and it has mainly been obtained from the polyaddition between polyisocyanates and polyols. Unfortunately, isocyanates such as toluene diisocyanate and methylene diphenyl diisocyanate are hazardous to both human health and the environment, and the phosgene used as the precursor of isocyanate is highly toxic. Due to these concerns, the use of non-isocyanate polyurethane (NIPU) has attracted great interest from academia and industry.

The synthesis of NIPU was first reported by Dyer and Scott in 1957, who found that cyclic carbonate reacted with amines to form urethane groups⁸. At present, this cyclic carbonate/amine reaction is still the most promising method for producing NIPU because of the optimal atom economy of 100%, the numerous choices for raw materials, and properties

that are analogous to traditional PU^{9,10}. The side hydroxyl groups that form from the cyclic carbonate/amine reaction increase the hydrogen bonding density to strengthen the mechanical properties and chemical resistance of NIPU¹¹⁻¹³. However, the cyclic carbonate possesses low reactivity with the amine¹⁴. This issue was addressed in our prior work, where we incorporated an epoxy chain extender, capitalizing on the elevated reaction rate between amine and epoxy¹⁵. Yet, in contrast, a majority of industrial epoxies originate from epichlorohydrin, which is considered to be a carcinogen and has been found to exhibit estrogenic effects on humans¹⁶. Hence, it is imperative to explore greener and more sustainable alternatives to increase the reactivity of cyclic carbonate for NIPU production.

Recently, vegetable oil has been one of the most promising materials to use for NIPU production, as its benefits include biodegradability, low cost, low toxicity, and low greenhouse emissions during production¹⁷⁻¹⁹. In addition, vegetable oil has a flexible long chain structure that allows it to act as a soft segment of PU. Moreover, the unsaturation and triglyceride groups of vegetable oil make it possible to be modified for PU synthesis and structure design²⁰. For example, the double bonds in vegetable oil can be epoxied followed by a ring opening to obtain bio-based polyol for the preparation of conventional PU²¹⁻²³. In an alternative process, vegetable oil could first be epoxied and then carbonated by CO₂ under catalysis to produce vegetable oil-based cyclic carbonate for the synthesis of NIPU^{24,25}. Zhang et al. prepared a plant oil-based cyclic carbonate by carbonating the epoxidized plant oil, subsequently yielding waterborne NIPUs²⁶. Nonetheless, akin to numerous NIPUs synthesized via the cyclic

carbonate ring-opening reaction, the resulting NIPU products typically necessitate a process that involves curing at relatively high temperatures and requires several days due to the formation of internal cyclic carbonate as well as steric hindrance arising from the long chain structure^{27–29}.

The thiol-ene reaction is another avenue for modifying vegetable oil and offers a high reaction rate and yield³⁰. Jia et al. modified tung oil to tung oil-based polyol through a thiol-ene reaction, then epoxied the polyol with epichlorohydrin to obtain a tung oil-derived epoxy plasticizer³¹. In another study, Mokhtari and co-workers synthesized jojoba and castor oil-based acids with a pendant carboxyl group through a thiol-ene reaction. These acids were then subjected to esterification to produce vegetable oil-based cyclic carbonates³². The synthesized cyclic carbonate displayed enhanced reactivity when reacted with an amine to synthesize NIPU, in comparison to cyclic carbonate obtained through the epoxidation/carbonation method. The enhanced reactivity can be attributed to the presence of pendant cyclic carbonate. However, because the NIPU synthesized from vegetable oil-based cyclic carbonates employed organic solvents, it was classified as a solvent-based NIPU.

Waterborne polyurethane has garnered considerable interest because it can achieve low volatile organic compounds. Waterborne polyurethanes are classified into three groups—cationic, anionic, and nonionic—based on the charge of the neutralized emulsifier. Although anionic and nonionic waterborne polyurethanes occupy most of the market, cationic waterborne polyurethanes demonstrate great application potential due to their excellent adhesion and

antibacterial properties, among other benefits^{33–35}. Therefore, the innovative aspect of this study lies in the synthesis of a cationic waterborne NIPU using a vegetable oil–based cyclic carbonate with higher reactivity, ultimately leading to reduced curing time.

In this paper, we describe the formulation of a series of waterborne NIPUs from a linseed oil–based cyclic carbonate featuring pendant cyclic carbonates in conjunction with bio-based fatty acid amine (FDA) and 3,3'-diamino-*N* methylpropylamine (DMDPA). Linseed oil, which is derived from flax seeds, is chosen as the precursor for chemical modification due to its eco-friendliness, sustainability, and high content of unsaturated double bonds. Herein, linseed oil is first reacted with thioglycolic acid to produce linseed oil acid (LOAC) through a thiol-ene reaction and is subsequently reacted with glycerol carbonate to produce linseed oil cyclic carbonate (LOCC), which harbors pendant cyclic carbonate groups. Different NIPU formulations were designed to tune the properties of the waterborne NIPU. The chemical structure of the LOCC was validated by Fourier transform infrared spectroscopy (FTIR) and ¹H and ¹³C nuclear magnetic resonance spectroscopy (NMR). The glass transition temperatures (T_g) of the NIPU coating films were characterized by differential scanning calorimetry (DSC), and their thermal stability was studied by thermogravimetric analysis (TGA). Viscoelastic and mechanical properties were determined using dynamic mechanical thermal analysis (DMTA) and tensile tests. General coating properties such as hardness, solvent resistance, impact resistance, and adhesion were also evaluated.

Experimental

Materials

Linseed oil, thioglycolic acid (98%, 92.12 g/mol), 1,1'-carbonyldiimidazole (CDI, $\geq 97.0\%$, 162.15 g/mol), 2,2'-azobis(2-methylpropionitrile) (AIBN) (98%, 164.21 g/mol), 3,3'-diamino-*N*-methyldipropylamine (96%, 145.25 g/mol⁻¹), sodium hydroxide (NaOH, $\geq 97.0\%$, 40.00 g/mol), methyl ethyl ketone (MEK) ($\geq 99.0\%$, 72.11 g/mol), and dichloromethane (CH₂Cl₂, $\geq 99.9\%$, 84.93 g/mol) were purchased from Sigma-Aldrich. Ethyl acetate ($\geq 99.5\%$, 88.106 g/mol) and magnesium sulfate (MgSO₄) were purchased from Fisher Scientific. Glycerol-1,2-carbonate ($\geq 90.0\%$, 118.09 g/mol), Sodium chloride (NaCl, $\geq 99.0\%$, 58.44 g/mol), and hydrochloric acid (HCl, 37%) were purchased from VWR International. Priamine™ 1075-LQ-(GD) dimer fatty acid diamine was provided by Croda International. The commercial waterborne PU (Varathane 200241H water-based ultimate polyurethane) was purchased from Amazon. All materials were used as received without further purification.

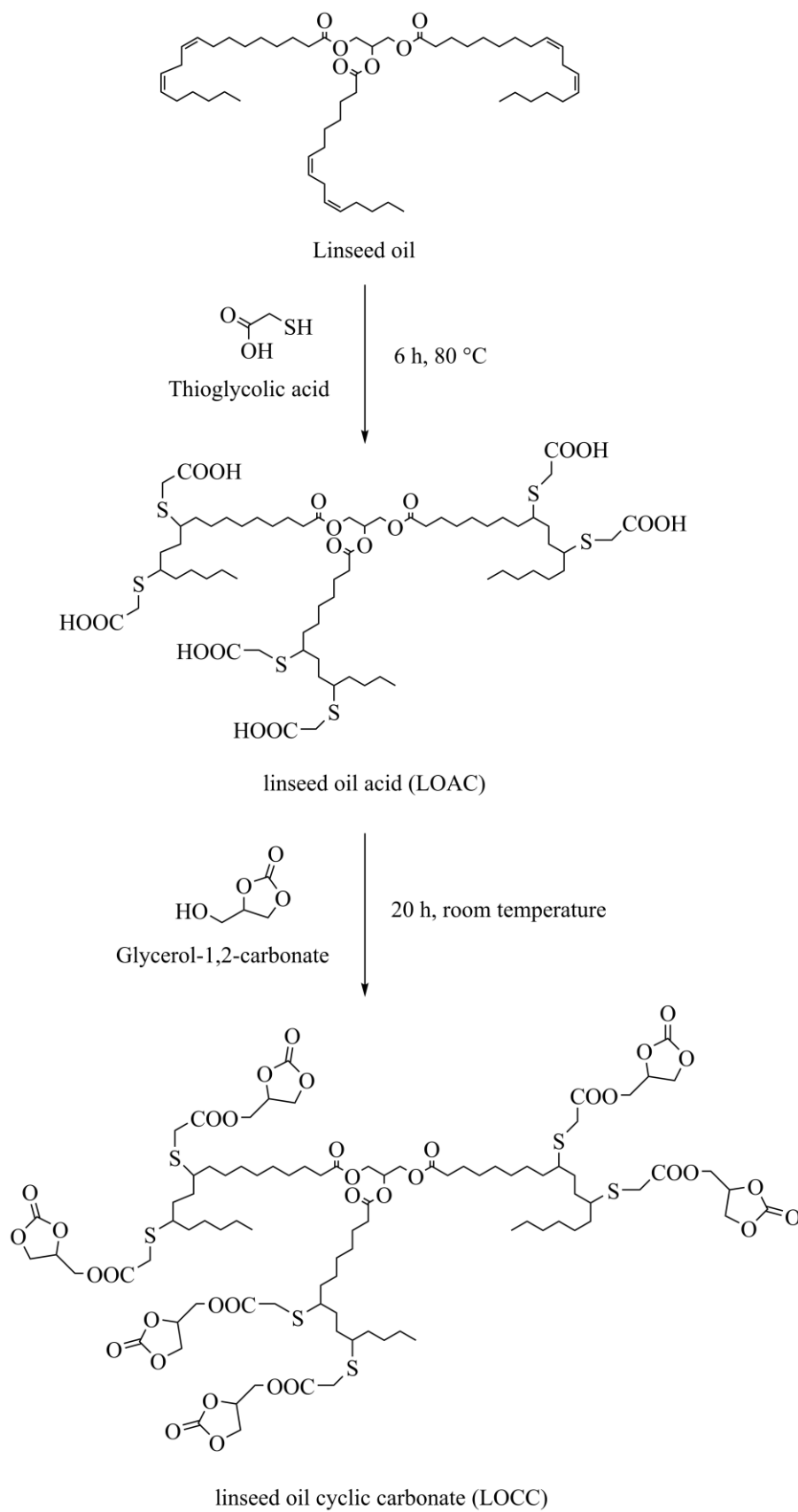
Synthesis procedure

Synthesis of linseed oil cyclic carbonate

The synthesis of linseed oil cyclic carbonate (LOCC) shown in Scheme 1 is similar to that in a previous report³². First, 70.0 g linseed oil and 7.78 g AIBN were mixed by magnetic stirring in an N₂ atmosphere. Next, 130.0 g of thioglycolic acid was dropped into the mixture to achieve a thiol/ene/AIBN molar ratio of around 3:1:0.1. The mixture was heated to 80 °C for 6 h to obtain linseed oil acid (LOAC). After the reaction, the product was dissolved in ethyl acetate

and washed three times with saturated NaCl solution. The organic layer was collected and then dried using magnesium sulfate, filtration, and solvent removal with a rotary evaporator.

The linseed oil cyclic carbonate (LOCC) was synthesized by the esterification between LOAC and glycerol carbonate. First, 35.0 g of LOAC was dissolved in CH_2Cl_2 in a three-neck round-bottom flask under N_2 purge. The flask was placed in an ice bath, and 38.8 g of 1,1'-carbonyldiimidazole (CDI) was added to the mixture. Next, 28.2 g of glycerol-1,2-carbonate was dropped into the flask for around 0.5 h. After the flask was removed from the ice bath, the mixture was permitted to react at room temperature for 20 h. The product was then collected by liquid-liquid extraction with ethyl acetate and was washed three times with 0.5 N HCl solution and 0.5 N NaOH solution. Finally, the organic layer was collected and dried using MgSO_4 , filtration, and solvent removal with a rotary evaporator.



Scheme 1. The synthesis procedure of LOCC.

Synthesis of solvent-borne NIPU

First, LOCC was dissolved in MEK followed by the addition of FDA. Next, the mixture was heated to 75 °C for 2 h. The product was named NIPU-1, and the formulation details are listed in Table 1. NIPU-1 was designed as a control to facilitate the comparison of its properties to those of waterborne NIPUs.

Synthesis of waterborne NIPU

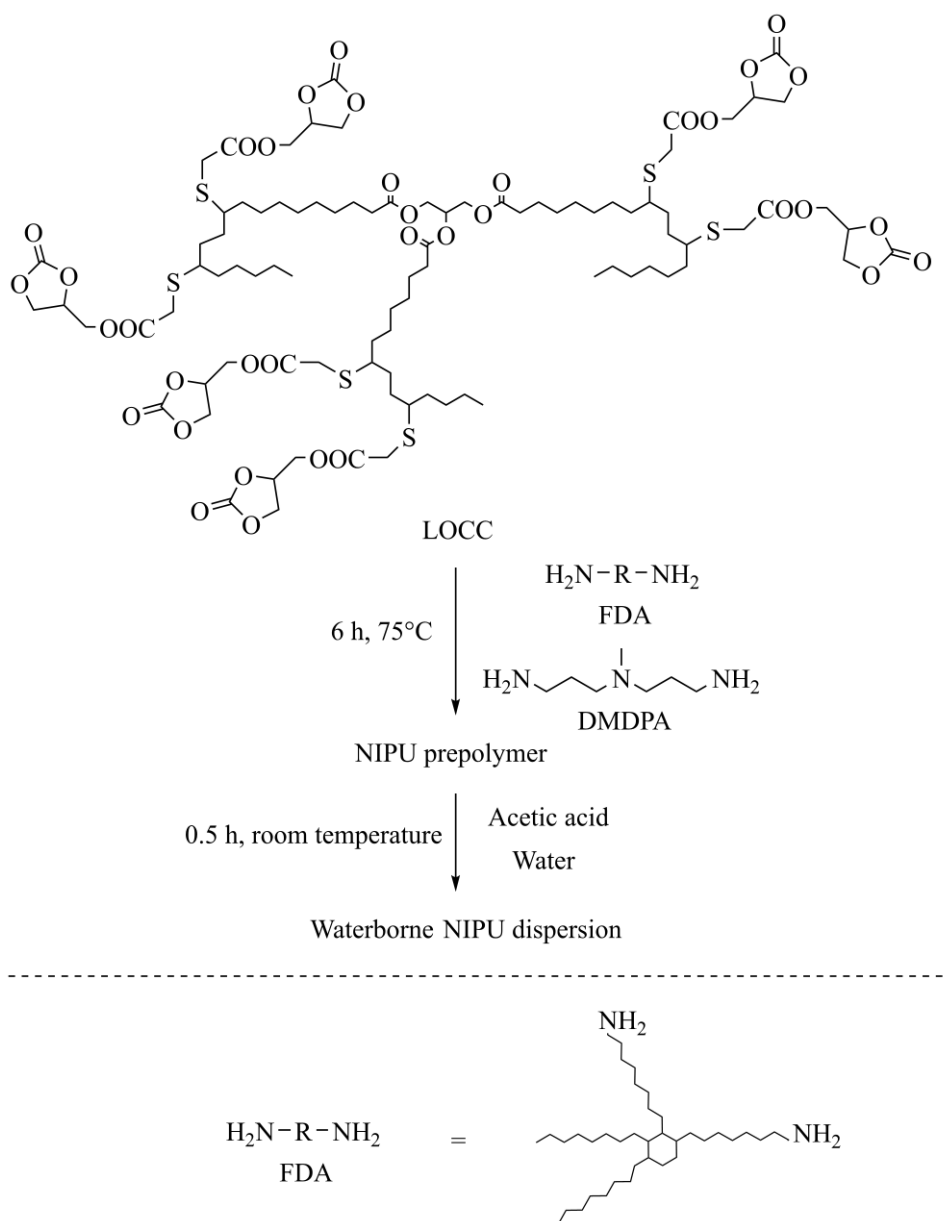
Three different waterborne NIPUs were designed by changing the content of the internal emulsifier (DMDPA), and their compositions are provided in Table 1. The molar ratio of the amine group to cyclic carbonate was kept at 1:1 for all NIPUs based on the theoretical functionality of LOCC. The synthesis procedure of the waterborne NIPUs is shown in Scheme 2. In this procedure, LOCC, FDA, and DMDPA were first mixed in MEK under an N₂ atmosphere, and the mixture was reacted at 75 °C for 6 h. Next, acetic acid with the same amount of DMDPA was added to the mixture to neutralize the product. After 0.5 h, the product was dispersed in water by a mechanical stirrer with a speed of 500 rpm for a period of 1 h, followed by solvent removal, which was accomplished using a rotary evaporator. The solid content of the dispersion was around 15–18 wt.%.

Table 1. The composition details of NIPU (wt.%).

	LOCC	FDA	DMDPA
NIPU-1	55	45	--
NIPU-2	63	32	5

NIPU-3	70	20	10
NIPU-4	78	7	15

Note: The molar ratio of cyclic carbonate to amine group is 1:1.



Scheme 2. The synthesis procedure of waterborne NIPU.

Preparation of NIPU coatings

After the synthesis of the NIPUs, the dispersions were applied on QD-36 steel substrates (Q-Lab Corporation) by a drawdown bar to a wet film thickness of 150 μm . The QD-36 substrates

were rinsed with acetone and were air-dried prior to use. The resulting samples were maintained at room temperature overnight before being cured at 120 °C for 6 h to form tack-free films. Once the coatings had cured, the dry film thickness was measured using an Elcometer digital coating thickness gauge.

Characterization methods

FTIR spectra for all samples were obtained by a Nicolet iS10 FTIR spectrometer at room temperature with an attenuated total reflection mode of 64 scans and a resolution of 4 cm⁻¹. The ¹H and ¹³C NMR spectra were obtained by a Varian INOVA 300 spectrometer at room temperature using CDCl₃ as the solvent.

The iodine values (i.e., the quantity of iodine, in grams, sufficient to react with 100 grams of a sample) of linseed oil and LOAC were determined according to the Wijs method using ISO 3961:2018. The acid value of LOAC was determined by acid–base titration, in which 0.3 g of LOAC was dissolved in 50 mL isopropyl alcohol, and 1 mL phenolphthalein (1% w/v) was dropped as an indicator. The resulting solution was titrated with 0.1 N potassium hydroxide (KOH). The acid value was calculated as:

$$A = \frac{56.1 \times V \times C}{W} \quad (1)$$

where A is the acid value (KOH g/g), V is the volume of titrant used, C is the molarity of the KOH solution, and W is the weight of the sample.

The carbonate equivalent weight (CEW) is the amount of product containing one equivalent of cyclic carbonate. The CEW was determined by the ^1H NMR spectra using benzophenone as the internal reference³⁶. Known amounts of benzophenone and LOCC were dissolved in 0.4 mL CDCl_3 in the NMR tube, and the CEW was determined using the equation below:

$$CEW = \frac{\int_{\text{benzophenone}}}{\int_{\text{cyclic carbonate}}} \times \frac{H_{\text{cyclic carbonate}}}{H_{\text{benzophenone}}} \times \frac{m_{\text{cyclic carbonate}}}{m_{\text{benzophenone}}} \times M_{\text{benzophenone}} \quad (2)$$

where $\int_{\text{benzophenone}}$ is the integration value of the proton signals of benzophenone at 7.4–7.7 ppm, $\int_{\text{cyclic carbonate}}$ is the integration value of cyclic carbonate signals at 4.9 ppm, $H_{\text{cyclic carbonate}}$ is the number of protons in α of the cyclic carbonate group, $H_{\text{benzophenone}}$ is the number of benzophenone protons, $m_{\text{cyclic carbonate}}$ is the weight of LOCC, $m_{\text{benzophenone}}$ is the weight of benzophenone, and $M_{\text{benzophenone}}$ is the molecular weight of benzophenone.

The stability of the waterborne NIPU dispersion was evaluated by centrifugation (Corning LSE compact centrifuge), which was conducted at 3000 rpm for 30 min. Dynamic light scattering using a Malvern ZetaSizer zeta potential analyzer was conducted at room temperature to investigate the particle size distribution of the waterborne NIPUs.

The glass transition temperature (T_g) of NIPU coating films was determined by differential scanning calorimetry (DSC; TA Instruments Q200) under a nitrogen atmosphere (40 mL min^{-1}) and at a rate of $10 \text{ }^\circ\text{C min}^{-1}$. The weight of the samples was around 5 mg. The temperature range was $-70 \text{ }^\circ\text{C}$ to $80 \text{ }^\circ\text{C}$.

The thermal stability of NIPU coating films was characterized by thermogravimetric analysis (TGA, TA Instruments Q500). The weight of the samples was around 10 mg. The temperature of each sample was raised to 600 °C at a steady rate of 10 °C min⁻¹ under nitrogen purge (10 mL min⁻¹), and the temperature was maintained at 600 °C for 10 minutes.

The viscoelastic properties of the cured coating films were examined using a TA Instruments Q800 dynamic mechanical thermal analyzer in tension mode with a constant frequency of 1 Hz. The tests were conducted on coating film that was peeled from the substrate and cut into samples that were 15 mm in length and 8 mm in width. The samples were cooled to -70 °C and heated to 80 °C at a rate of 3 °C min⁻¹.

The mechanical properties of NIPU coating films were tested using an Instron 5567 universal testing machine (Instron Corp.) operated at room temperature. Self-standing films were peeled from the substrates and were cut into the desired dimensions for mechanical testing (approximately 30 mm in length and 10 mm in width). The moving speed of the test frame was 5 mm min⁻¹. The average obtained by testing five replicates of each sample is reported.

The viscosity of the polyurethane dispersions was measured using an ARES-G2 rheometer (TA Instruments) with a 25-mm cone-and-plate geometry. The measurement was carried out at 25 °C, using a shear rate ranging from 1 s⁻¹ to 100 s⁻¹. The NIPU coating samples (i.e., the coatings on the steel substrates) were also evaluated for their general coating properties. Other

properties that were investigated and the standards that were used included pendulum hardness (ASTM D4366), pencil hardness (ASTM D3363), solvent resistance (ASTM D4752), reverse impact resistance (ISO 6272-2), crosshatch adhesion (ASTM D3359), and pull-off adhesion (ASTM D4541).

Results and discussion

Characterization of linseed oil acid and linseed oil cyclic carbonate

The synthesis of linseed oil cyclic carbonate (LOCC) involves two steps. The first step is the functionalization of linseed oil with thioglycolic acid to obtain linseed oil acid (LOAC) by thiol-ene click reaction. Here, a thiol/ene molar ratio of 3:1 was selected to obtain the best yield³⁷. The iodine values obtained for linseed oil and LOAC were 174 g/100 g and 1.1 g/100 g, respectively. The acid value of LOAC was also determined based on the titration, and the obtained acid value of 0.25 KOH g/g is in good agreement with the theoretical acid value (0.24 KOH g/g). The second step in the synthesis is the esterification of LOAC with glycerol-1,2-carbonate catalyzed by CDI to obtain LOCC.

The successful synthesis of LOAC and LOCC was further confirmed by both FTIR and NMR spectra. In the FTIR spectra presented in Fig. 1, the peak at 3010 cm^{-1} in the linseed oil curve was attributed to double bond stretching, while the peaks at 2923 cm^{-1} and 2853 cm^{-1} were assigned to C-H stretching, and the signal at 1742 cm^{-1} was assigned to the C=O stretching of ester³⁸. After the conversion of the linseed oil to LOAC, the signal for double bond stretching

at 3010 cm^{-1} disappeared, and a new signal appeared at 1708 cm^{-1} that was associated with the C=O stretching of acid. In addition, after the esterification of LOAC, a new peak appeared at 1798 cm^{-1} in the LOCC curve, and this peak was associated with the C=O stretching of cyclic carbonate³⁹.

Nuclear magnetic resonance spectroscopy (both ^1H NMR and ^{13}C NMR) also confirmed the chemical structures of the LOAC and LOCC. As shown in Fig. 2 (a), the peak in the spectrum for linseed oil at 5.35 ppm belongs to the vinyl protons; this peak disappears in the spectrum for LOAC, as shown in Fig. 2 (b), and two new peaks are generated: one at 2.75 ppm that corresponds to the proton in CH-S and another at 3.21 ppm that corresponds to the proton linked to the acid group^{37,40}. The spectrum for LOCC, shown in Fig. 2 (c), exhibits peaks at 4.96, 4.57, and 4.26–4.46 ppm that are associated with the protons of cyclic carbonate. The equivalent weight of the cyclic carbonate was also characterized by ^1H NMR, and the carbonate equivalent weight of LOCC was 351 g/eq. Given the theoretical molecular weight of LOCC (1988 g/mol), the functionality of LOCC was determined to be 5.7. Fig. S1 (a) shows the ^{13}C NMR spectra of LOAC, which exhibits peaks at 47 ppm (attributed to carbon signals near the carboxyl group) and 176 ppm (attributed to the carboxyl group). Fig. S1 (b) shows the ^{13}C NMR spectra of LOCC, the peaks at 74, 66, 154, and 171 ppm are associated with the signals of carbons on the cyclic carbonate and the ester. Taken together, the FTIR and NMR characterization results demonstrate that the LOAC and LOCC were successfully synthesized.

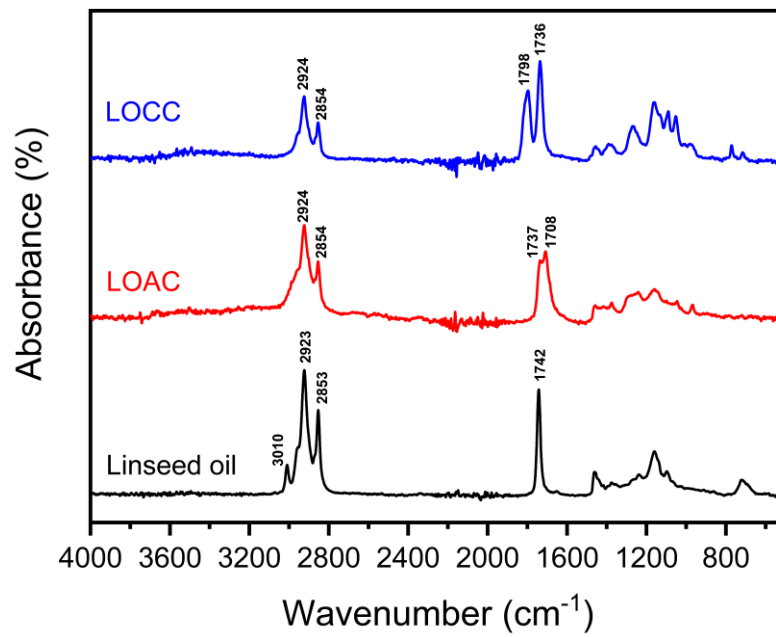


Fig. 1. FTIR spectra of linseed oil, LOAC, and LOCC.

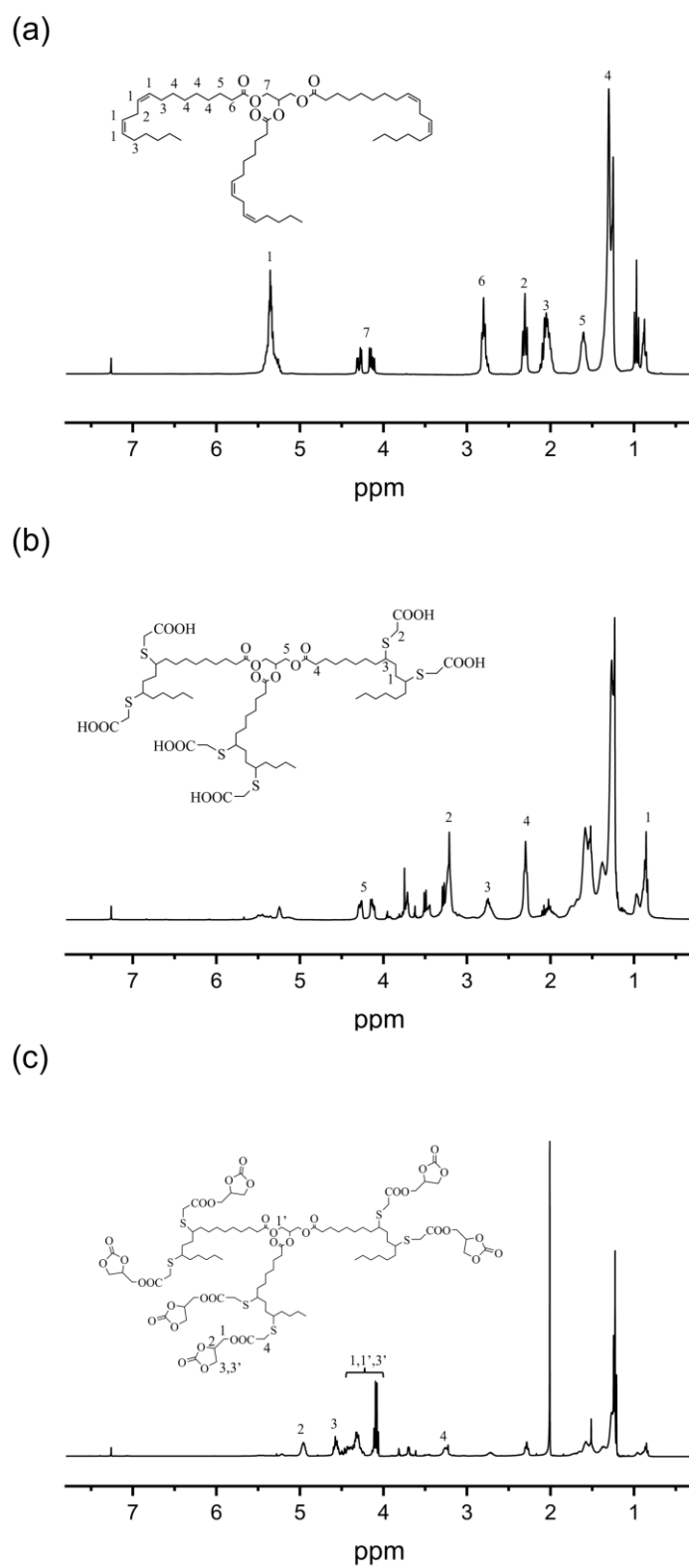


Fig. 2. ^1H NMR spectra of (a) linseed oil, (b) LOAC, and (c) LOCC.

Conversion of cyclic carbonates in linseed oil cyclic carbonate

Before being dispersed into the water, linseed oil cyclic carbonate (LOCC) was reacted with DMDPA and FDA at 75 °C for 6 h to obtain the NIPU prepolymer. The FTIR spectra of the mixture obtained before and after the cyclic carbonate–amine reaction are shown in Fig. S2. The conversion of the cyclic carbonate groups was estimated based on the area of the C=O stretching peak of cyclic carbonate at 1798 cm⁻¹. The peaks of C-H stretching at 2923 and 2853 cm⁻¹ were chosen as the internal reference. The conversion of cyclic carbonate was calculated using the following formula:

$$C = 1 - \frac{A_1/A_H}{A_0/A_H} \times 100 \quad (3)$$

where C is the conversion of cyclic carbonate; A_0 and A_1 are the peak areas of the cyclic carbonate functional group before and after the reaction, respectively; and A_H is the area of the peaks of C-H stretching. The values obtained for the conversion of the cyclic carbonate in NIPU-1, NIPU-2, NIPU-3, and NIPU-4 after the cyclic carbonate-amine reaction were 15.0%, 19.6%, 37.2%, and 44.1%, respectively.

Storage stability and particle size of NIPU dispersion

In this study, one solvent-borne NIPU and three waterborne NIPU dispersions were prepared. The average particle sizes for the three waterborne NIPU dispersions ranged from 115 to 136 nm, as shown in Fig. S3. The storage stability of a waterborne NIPU dispersion was determined if sedimentation was observed during storage at room temperature. The results showed that NIPU-3 and NIPU-4 did not show any sedimentation after 3 months, whereas

NIPU-2 showed sedimentation within 1 month. Moreover, no sedimentation was observed for NIPU-3 and NIPU-4 when centrifuged at 3000 rpm for 30 min, while sedimentation was evident for NIPU-2. For NIPU-3 and NIPU-4, more DMDPA was incorporated into the coating system; therefore, after neutralization, more ions were present at the particle surface, and these ions improved the hydrophilicity and stability of the coating⁴¹.

Characterization of NIPU films

After baking at 120 °C for 6 h, touch-free films were produced from the solvent-borne NIPU and the three different waterborne NIPU formulations. FTIR was adopted to characterize all four films, and the results are shown in Fig. 3. By comparing the FTIR spectra of the NIPU films in this figure with that for LOCC (Fig. 1), it can be noticed that new broad peaks were formed at 3600–3200 cm⁻¹ that are associated with the O-H stretching and N-H stretching, which resulted from the reaction between amine and cyclic carbonate (Fig. 3). The peak for LOCC at 1798 cm⁻¹ assigned to the C=O stretching of cyclic carbonate vanished, and a new peak at 1710 cm⁻¹ appeared in the spectra of the NIPU films, corresponding to the C=O stretching of the urethane group^{42,43}. The disappearance and appearance of these typical signals confirmed the consumption of LOCC and the formation of NIPU.

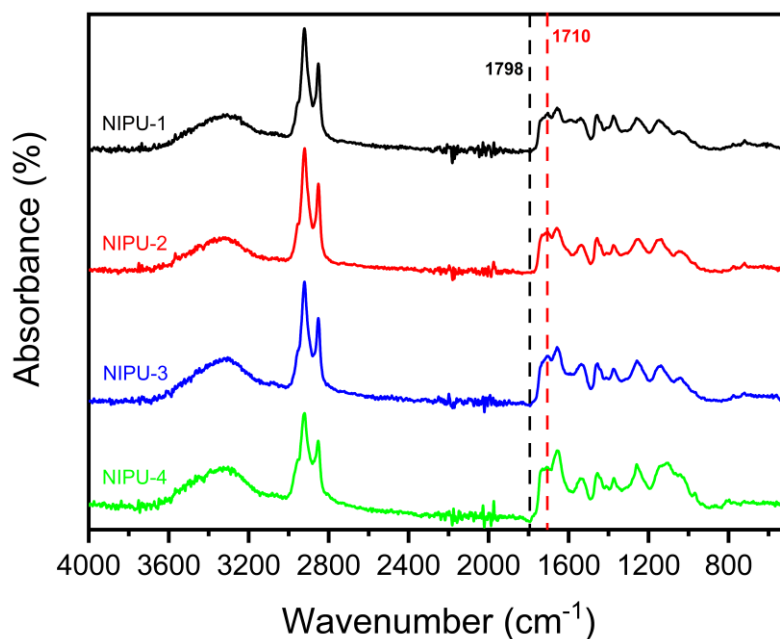


Fig. 3. FTIR spectra of the NIPU coating films (composition details are provided in Table 1).

Glass transition temperature

The glass transition temperature (T_g) of NIPU coating films was investigated by DSC. In the DSC curves presented in Fig. 4 (a), only one T_g was identified for each NIPU sample, and the derivative DSC curve (shown in Fig. 4 (b)) further confirmed this observation⁴⁴. Moreover, within the testing temperature range, no other characteristic signal was observed, which implies an amorphous structure for the NIPU films and indicates that all of the functional groups in the films were fully reacted.

The T_g values obtained for NIPU-1, NIPU-2, NIPU-3, and NIPU-4 were -9 , 0 , 6 , and 11 °C, respectively. Based on these results, it is obvious that the T_g has increased with the increase in DMDPA content. This result is attributed to the reduced chain mobility for shorter chains as

compared to that for longer chains. In addition, the higher DMDPA content results in a higher urethane group content, which leads to more hydrogen bonding⁴⁴. Therefore, a higher T_g was found for NIPU films with higher DMDPA contents.

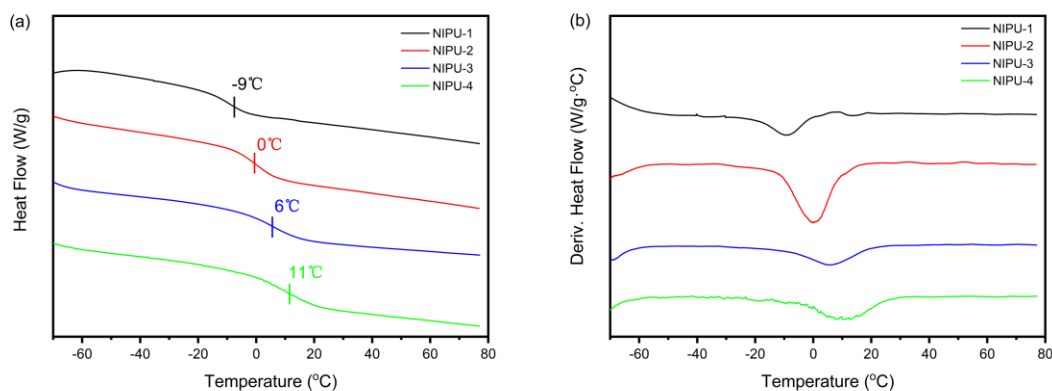


Fig. 4. (a) DSC curves and (b) derivative DSC curves for NIPU coating films (composition details are provided in Table 1).

Mechanical and thermal properties of NIPU films

DMTA analysis was utilized to investigate the viscoelastic properties of the NIPU films. Fig. 5 shows the storage modulus and loss factor as a function of temperature, where T_g is the temperature at which the loss factor was maximum within the temperature range. Table 2 lists the T_g and storage modulus within the glassy region (i.e., E' at -25 °C). The T_g obtained from DMTA shows the same trend as that obtained from the DSC results. The difference in the T_g results obtained from DSC and DMTA for the same NIPU film is attributed to the different testing methods.

The storage modulus describes the elasticity of materials. From Table 2, the E' value for the solvent-borne NIPU film (i.e., NIPU-1) was 1023 MPa, but the E' value for the waterborne

film NIPU-2 was only 696 MPa. Solvent-borne coatings show better performance than waterborne coatings because of the differences in the film formation processes. For solvent-borne coatings, film formation occurs in a homogeneous phase that leads to a uniform film. However, film formation for waterborne coatings takes place in two inhomogeneous phases (a liquid phase and a solid phase), which may increase the chance to generate defects in the films^{45,46}. For waterborne coatings, increasing the LOCC content results in a gradual increase in E' from 696 (in NIPU-2) to 1194 Mpa (NIPU-4).

The elongation-at-break (ϵ), tensile strength (σ), and Young's modulus E for the NIPU coating films are listed in Table 3. The elongation-at-break decreased with the increase in LOCC and DMDPA content (from NIPU-1 to NIPU-4). The tensile strength and Young's modulus for NIPU-1 were slightly higher than those for NIPU-2; this may result from the formation of a film with fewer defects for the solvent-borne coating during the curing process. For the waterborne coatings, the σ and E changed from 0.32 and 0.26 MPa, respectively (for NIPU-2) to 0.55 and 0.82 MPa, respectively (for NIPU-4). The reason for the improved toughness of the polymer films is attributed to the higher content of urethane groups, which leads to more hydrogen bonding, thus increasing the physical cross-linking. In addition, the higher content of DMDPA also improves the polarity of the polyurethane, leading to higher mechanical strength⁴⁷. Therefore, higher values for the storage modulus, σ , and E as well as lower values for elongation-at-break were observed for NIPU-4 than for NIPU-3 and NIPU-2.

Table 2. Glass transition temperature (T_g) and storage modulus (E') of the NIPU coatings from DMTA.

	T_g (°C)	E' (MPa)
NIPU-1	2	1023
NIPU-2	23	696
NIPU-3	28	769
NIPU-4	34	1194

The thermal stability of the NIPU films was characterized by TGA, and the results are shown in Fig. 6. All NIPU films began decomposing at 220 °C and were fully decomposed at approximately 500 °C. The temperatures at 10% and 20% weight loss are also listed in Table 3. For NIPU-1, T_{10} and T_{20} were 274 °C and 346 °C, respectively; however, for NIPU-2, the values were slightly higher. T_{10} and T_{20} then decreased to 253 °C and 297 °C, respectively, for NIPU-4. The reduction of T_{10} and T_{20} from NIPU-2 to NIPU-4 could be explained by the different contents of urethane groups in the waterborne NIPU films. NIPU-4 was incorporated into more cyclic carbonate, which resulted in the formation of more urethane groups upon curing. Since urethane groups tend to decompose first under elevated temperatures, a NIPU with a higher content of urethane groups would be more easily decomposed³⁹. In general, NIPU-1 (the solvent-borne NIPU) has a thermal stability that is higher than NIPU-3 and NIPU-4 but is comparable to that for NIPU-2. NIPU-2 has a similar thermal stability and an even higher T_{10} than NIPU-1, which may be due to the combined contributions from hydrogen bonding and urethane group content⁴⁸.

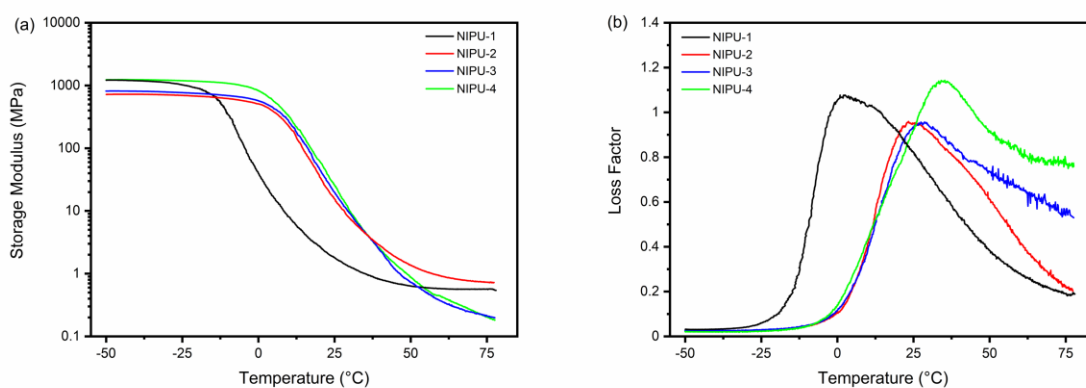


Fig. 5. (a) Storage modulus and (b) loss factor for the NIPU coating films.

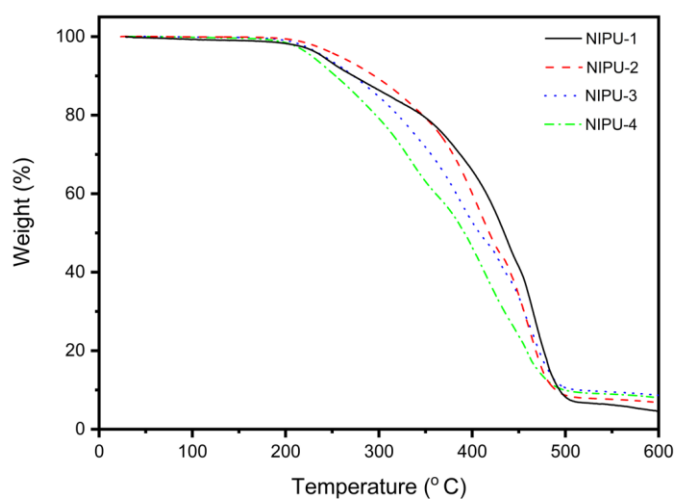


Fig. 6. TGA curves for the NIPU coating films.

Table 3. Thermal and mechanical properties of the NIPU coating films.

	TGA (°C)		Tensile test results		
	T_{10}	T_{20}	ε (%)	σ (MPa)	E (MPa)
NIPU-1	273	346	144.1±12.2	0.39±0.04	0.27±0.03
NIPU-2	295	347	119.5±14	0.32±0.04	0.26±0.03
NIPU-3	273	320	89.6±15.5	0.41±0.14	0.46±0.09

NIPU-4	253	297	68.3±16.1	0.55±0.14	0.82±0.16
--------	-----	-----	-----------	-----------	-----------

General coating properties

General coating properties of the synthetic NIPUs and commercial waterborne polyurethane (WPU) coating films—including pendulum hardness, pencil hardness, solvent resistance, impact resistance, crosshatch adhesion, and pull-off adhesion—are listed in Table 4. The viscosity of the coatings is presented in Fig. S4. A commercial WPU with 27.4% solid content (Varathane 200241H Water-Based Ultimate Polyurethane) was purchased from Amazon. The commercial WPU was drawn down on the steel substrate with a wet film thickness of 120 μm , and it was cured overnight at room temperature. All coatings showed very high solvent resistance and impact resistance. In terms of hardness (pendulum hardness and pencil hardness), all NIPU samples showed hardness values that were similar but were much lower than that of the commercial WPU. The NIPU coating samples showed very strong adhesion to the steel panels (both crosshatch adhesion and pull-off adhesion), while the commercial WPU exhibited much lower adhesion. The waterborne NIPU coatings (NIPU-2, NIPU-3, and NIPU-4) showed comparable performance to the commercial WPU; although they are softer than the commercial formulation, they presented better adhesion. The waterborne NIPU coatings also showed better reverse impact resistance than the commercial WPU, with a 200+ kg·cm impact resistance. Overall, the waterborne NIPU coatings performed as well as the solvent-borne NIPU coating (NIPU-1) in terms of hardness, solvent resistance, impact resistance, and adhesion.

Table 4. General coating properties of the NIPU coating films.

	Dry film thickness (μm)	Pendulum hardness (s)	Pencil hardness	Solvent resistance	Reverse impact resistance ($\text{kg}\cdot\text{cm}$)	Crosshatch adhesion*	Pull-off adhesion (MPa)
NIPU-1	47.9	11	4B	100+	200+	4B	1.3 ± 0.2
NIPU-2	49.5	12	4B	100+	200+	4B	1.4 ± 0.1
NIPU-3	50.0	15	4B	100+	200+	4B	1.4 ± 0.1
NIPU-4	51.5	13	4B	100+	200+	4B	1.5 ± 0.2
Commercial WPU	57.3	53	HB	100+	100+	0B	0.4 ± 0.1

*Crosshatch adhesion values range from 0B (worst) to 5B (best).

Conclusion

In this study, linseed oil-based waterborne NIPU coatings having a substantial bio-based content were successfully designed and synthesized. The linseed oil was transformed to linseed oil cyclic carbonate through a thiol-ene reaction followed by esterification. The cyclic carbonate was then reacted with bio-based FDA and DMDPA to obtain waterborne NIPU coatings with high bio-based content. By controlling the content of DMDPA, variation in the urethane content was induced. The resulting NIPU coatings showed different storage stabilities, particle size distributions, thermal properties, and mechanical properties. For waterborne NIPU coatings, the samples having higher DMDPA content showed better storage stability and more uniform particle size distributions. In addition, after curing, the coating films with higher DMDPA content showed higher T_g and mechanical strength but lower elongation and thermal stability. Despite the lower DMDPA content, the solvent-borne NIPU coating demonstrated

superior mechanical properties to those for the waterborne coating NIPU-2. This finding can be attributed to the distinctions in the dispersant environment. Nevertheless, by adjusting the formulation, it was possible to produce waterborne NIPU coatings with properties that are comparable to those of the solvent-borne NIPU coating in terms of adhesion, solvent resistance, impact resistance, and hardness. The successful synthesis of highly bio-based waterborne NIPU underscores the potential of utilizing vegetable oils in NIPU coatings and paves the way for a novel direction in the advancement of vegetable oil-based waterborne NIPU coatings.

Acknowledgment

The authors acknowledge the support from the U.S. National Science Foundation (NSF CAREER Award, #1943860). The authors appreciate the technical support from Dr. Lingyan Li at the National Center for Education and Research on Corrosion and Materials Performance. The authors also appreciate Sheila Pearson for her invaluable assistance in editing and proofreading this manuscript.

SUPPORTING INFORMATION

The supporting information is available free of charge. This information includes ^{13}C NMR spectra for LOAC and LOCC, FTIR spectra of NIPU prepolymer, the particle size distributions of waterborne NIPU dispersions, and viscosity of NIPU dispersions and commercial WPU.

Reference

- 1 L. Zhang, Y. Huang, H. Dong, R. Xu and S. Jiang, *Compos B Eng*, 2021, **223**, 109149.
- 2 Y. Yue, X. Gong, W. Jiao, Y. Li, X. Yin, Y. Si, J. Yu and B. Ding, *J Colloid Interface Sci*, 2021, **592**, 310–318.
- 3 C. Shen, Y. Cao, J. Rao, Y. Zou, H. Zhang, D. Wu and K. Chen, *Food Packag Shelf Life*, 2021, **29**, 100721.
- 4 H. Haridevan, D. A. C. Evans, A. J. Ragauskas, D. J. Martin and P. K. Annamalai, *Green Chemistry*, 2021, **23**, 8725–8753.
- 5 S. Li, S. Wang, X. Du, H. Wang, X. Cheng and Z. Du, *Prog Org Coat*, 2022, **163**, 106613.
- 6 Polyurethane Market Size, Growth & Trends Report, 2022-2030, <https://www.grandviewresearch.com/industry-analysis/polyurethane-pu-market>, (accessed 28 July 2022).
- 7 P. Król, *Prog Mater Sci*, 2007, **52**, 915–1015.
- 8 E. Dyer, H. Scott Vol, B. Elizabeth Dyer and H. Scott, *J Am Chem Soc*, 1957, **79**, 672–675.
- 9 X. Yang, S. Wang, X. Liu, Z. Huang, X. Huang, X. Xu, H. Liu, D. Wang and S. Shang, *Green Chemistry*, 2021, **23**, 6349–6355.
- 10 G. Coste, D. Berne, V. Ladmiral, C. Negrell and S. Caillol, *Eur Polym J*, 2022, **176**, 111392.
- 11 B. Quienne, R. Poli, J. Pinaud and S. Caillol, *Green Chemistry*, 2021, **23**, 1678–1690.
- 12 I. Javni, D. Hong, Z. P.-J. of A. Polymer and undefined 2008, *Wiley Online Library*, 2008, **108**, 3867–3875.
- 13 Y. Ecochard and S. Caillol, *Eur Polym J*, 2020, **137**, 109915.
- 14 C. Carré, Y. Ecochard, S. Caillol and L. Avérous, *ChemSusChem*, 2019, **12**, 3410–3430.
- 15 C. Zhang, H. Wang and Q. Zhou, *Green Chemistry*, 2020, **22**, 1329–1337.
- 16 I. A. for R. on Cancer, 1999, 928–928.
- 17 H. Khatoon, S. Iqbal, M. Irfan, A. Darda and N. K. Rawat, *Prog Org Coat*, 2021, **154**, 106124.
- 18 M. A. R. Meier, J. O. Metzger and U. S. Schubert, *Chem Soc Rev*, 2007, **36**, 1788–1802.
- 19 M. A. Mosiewicki and M. I. Aranguren, *Eur Polym J*, 2013, **49**, 1243–1256.
- 20 I. Babahan-Bircan, J. Thomas and M. D. Soucek, *Journal of Coatings Technology and Research 2022*, 2022, 1–16.
- 21 L. Hojabri, X. Kong and S. S. Narine, *Biomacromolecules*, 2009, **10**, 884–891.
- 22 X. Kong, G. Liu, H. Qi and J. M. Curtis, *Prog Org Coat*, 2013, **76**, 1151–1160.
- 23 C. Zhang, H. Liang, D. Liang, Z. Lin, Q. Chen, P. Feng and Q. Wang, *Angewandte Chemie International Edition*, 2021, **60**, 4289–4299.
- 24 A. Lee and Y. Deng, *Eur Polym J*, 2015, **63**, 67–73.
- 25 X. Yang, C. Ren, X. Liu, P. Sun, X. Xu, H. Liu, M. Shen, S. Shang and Z. Song, *Mater Chem Front*, 2021, **5**, 6160–6170.

- 26 W. Zhang, T. Wang, Z. Zheng, R. L. Quirino, F. Xie, Y. Li and C. Zhang, *Chemical Engineering Journal*, 2023, **452**, 138965.
- 27 X. Liu, X. Yang, S. Wang, S. Wang, Z. Wang, S. Liu, X. Xu, H. Liu and Z. Song, *ACS Sustain Chem Eng*, 2021, **9**, 4175–4184.
- 28 S. Doley and S. K. Dolui, *Eur Polym J*, 2018, **102**, 161–168.
- 29 A. Cornille, R. Auvergne, O. Figovsky, B. Boutevin and S. Caillol, *Eur Polym J*, 2017, **87**, 535–552.
- 30 C. E. Hoyle and C. N. Bowman, *Angewandte Chemie International Edition*, 2010, **49**, 1540–1573.
- 31 P. Jia, Y. Ma, H. Xia, M. Zheng, G. Feng, L. Hu, M. Zhang and Y. Zhou, *ACS Sustain Chem Eng*, 2018, **6**, 13983–13994.
- 32 C. Mokhtari, F. Malek, A. Manseri, S. Caillol and C. Negrell, *Eur Polym J*, 2019, **113**, 18–28.
- 33 X. He, J. He, Y. Sun, X. Zhou, J. Zhang and F. Liu, *J Coat Technol Res*, 2022, **19**, 1055–1066.
- 34 N. Sukhawipat, N. Saetung, P. Pasetto, J. F. Pilard, S. Bistac and A. Saetung, *Prog Org Coat*, 2020, **148**, 105854.
- 35 Y. Zhang, W. Zhang, H. Deng, W. Zhang, J. Kang and C. Zhang, *ACS Sustain Chem Eng*, 2020, **8**, 17447–17457.
- 36 B. Quienne, R. Poli, J. Pinaud and S. Caillol, *Green Chemistry*, 2021, **23**, 1678–1690.
- 37 M. Desroches, S. Caillol, V. Lapinte, R. Auvergne and B. Boutevin, *Macromolecules*, 2011, **44**, 2489–2500.
- 38 K. Li, Z. Liu, C. Wang, W. Fan, F. Liu, H. Li, Y. Zhu and H. Wang, *Prog Org Coat*, 2020, **145**, 105668.
- 39 Z. Ling, C. Zhang and Q. Zhou, *Prog Org Coat*, 2022, **169**, 106915.
- 40 S. Malburet, C. Di Mauro, C. Noè, A. Mija, M. Sangermano and A. Graillot, *RSC Adv*, 2020, **10**, 41954–41966.
- 41 X. Wang, H. Liang, J. Jiang, Q. Wang, Y. Luo, P. Feng and C. Zhang, *Green Chemistry*, 2020, **22**, 5722–5729.
- 42 C. Zhang, H. Wang and Q. Zhou, *Green Chemistry*, 2020, **22**, 1329–1337.
- 43 K. Huang, Z. Ling and Q. Zhou, *Journal of Composites Science 2021, Vol. 5, Page 194*, 2021, **5**, 194.
- 44 Q. M. Jia, M. Zheng, Y. C. Zhu, J. B. Li and C. Z. Xu, *Eur Polym J*, 2007, **43**, 35–42.
- 45 E. Brinkman and P. Vandevoorde, *Prog Org Coat*, 1998, **34**, 21–25.
- 46 A. Wegmann, *Prog Org Coat*, 1997, **32**, 231–239.
- 47 P. Król, *Prog Mater Sci*, 2007, **52**, 915–1015.
- 48 G. Vogt, S. Woell and P. Argos, *J Mol Biol*, 1997, **269**, 631–643.